Applied Catalysis B: Environmental 230 (2018) 77–90

Contents lists available at ScienceDirect

Applied Catalysis B: Environmental

journal homepage: www.elsevier.com/locate/apcatb

Advanced oxidation process for the removal of ibuprofen from aqueous solution: A non-catalytic and catalytic ozonation study in a semi-batch reactor

Soudabeh Saeid[a], Pasi Tolvanen[a], Narendra Kumar[a], Kari Eränen[a], Janne Peltonen[c], Markus Peurla[c], Jyri-Pekka Mikkola[a,b], Andreas Franz[a], Tapio Salmi[a,*]

[a] Laboratory of Industrial Chemistry and Reaction Engineering, Johan Gadolin Process Chemistry Centre, Åbo Akademi University, Biskopsgatan 8, FI-20500, Åbo/Turku, Finland
[b] Technical Chemistry Department of Chemistry Chemical-Biological Center, Umeå University, SE-90187, Umeå, Sweden
[c] University of Turku, Laboratory of Electron Microscopy, Department of Industrial Physics and Astronomy, FI-20540, Turku, Finland

ARTICLE INFO

Keywords:
Ibuprofen
Ozone
Advanced oxidation processes (AOPs)
Heterogeneous catalyst

ABSTRACT

The Concern on the availability of clean and safe fresh water and the quality of recycled wastewater are important issues, which require a suitable technology to restore the water quality. Pharmaceuticals in waste water are not easily degraded by conventional water treatment technology. Advanced oxidation processes have been applied to eliminate traces of these compounds from aquatic environments. This study was focused on the degradation of ibuprofen (IBU) in aqueous solutions by catalytic and non-catalytic ozonation. Preliminary experiments were conducted to optimize the ozone concentration in water and to investigate other operation parameters. The operation parameters were: temperature, stirring rate, gas flow rate, pH, and use of Spinchem stirrer to reach higher concentrations of dissolved ozone. In general, the initial concentration of IBU was 10 mg/L, and about 93% of IBU was degraded after 4 h of ozonation under optimal conditions. Additional experiments were carried out to investigate the benefit of applying a solid catalyst. H-Beta and Fe-H-Beta type catalysts were immobilized in the Spinchem rotating bed device. The catalytic experiments illustrated a significant improvement in the degradation rate of IBU. The catalysts were characterized by nitrogen adsorption- desorption, scanning electron microscopy, transmission electron microscopy, X-ray powder diffraction and FTIR.

1. Introduction

Freshwater resources are continuously influenced by municipal and industrial pollutants. Increasing chemical contamination and disinfection by products have created a large concern during the recent years. Implementation of environmentally clean and safe chemical technologies, processes and materials are necessary for maintaining the water quality and controlling the water pollution [1–3]. Among the huge amount of diverse organic waste products, pharmaceutical compounds remain in surface water and groundwater. The consumption of pharmaceuticals increase worldwide, and they are active at very low concentrations, which becomes a major concern as it cause risks to the human health and environment [4,5]. Common technologies have been used for the pharmaceutical wastewater treatment. Within conventional methods, such as sewer or direct disposal, wastewater is disposed into rivers and seas. Recent studies reveal that an adequate removal of pharmaceutical compounds is not possible through conventional techniques [6,7].

Pharmaceutical compounds which are mostly released by human and animal excretion can enter the water sources. IBU is an efficient pharmaceutical for relieving pain and reducing fever. Because it relieves pain effectively in almost the whole human body, It is used as a reliever for fever symptoms, menstrual cramps, headaches, arthritis, and many other common pains [8]. The molecular structure of IBU is displayed in Fig. 1.

Ibuprofen (IBU) is a member of the propionic acid group in the Non-steroidal anti-inflammatory drugs (NSAID's) class [6]. EC_{50} values are commonly used in environmental toxicology: algae, daphnia and fish as bioassays. According to the OECD guideline, the toxicity values (EC50) of ibuprofen for the species *Scenedesmus abundans* (water green microalgae) and *Daphnia similis* (common water flea) are 1170 μg/L and 97,000 μg/L, respectively [9,10]. IBU has been identified in a broad range of concentrations in landfill leachate, groundwater, and surface waters. A number of rivers in Europe report concentrations of IBU, for

* Corresponding author.
E-mail address: tapio.salmi@abo.fi (T. Salmi).

https://doi.org/10.1016/j.apcatb.2018.02.021
Received 9 August 2017; Received in revised form 22 January 2018; Accepted 9 February 2018
Available online 21 February 2018
0926-3373/

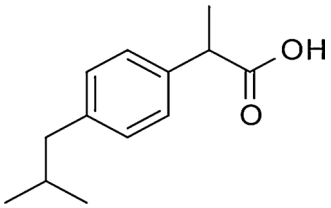

Fig. 1. Structural formula of ibuprofen (IBU).

instance in Aura river,Turku, Finland around 20 μg/L, in river Thames, London, UK, around 0.783 μg/L, in smallrivers in UK around 2 μg/L, whereas in river Rakkolanjoki, Finland, a seasonal variation isobserved −0.15 μg/L in February and 0.35 μg/L in May [11–14].

Even low concentrations of IBU can affect the aquatic ecosystem i.e. the accumulation of IBU in food chains can result in a significant influence on the human health and living creatures. For example, the survival of Japanese rice fish (*Oryzias latipes*) can be critical at very low IBU concentrations of 0.0001 mg/L. For this species, IBU can influence on the estrogen homeostasis and thus damage the reproduction [15]. Although IBU has been identified in drinking and surface waters in UK, IBU was found to have 49.5% risk characterization ratio (RCR) in rivers of UK, which according to the study of Boxall et al. is identified as an unacceptable environmental risk [16–18]. It is similarly harmful for the kidney function, an endocrine disruptor, and harms the regeneration in teleostei fish. Also, it may result in hampered embryo movement and hatching in zebrafish [19].

IBU is poorly attenuated by conventional water treatment techniques. Therefore, it is necessary to develop a new and efficient method for removing IBU. A variety of analytical techniques for the determination of IBU such as potentiometric titration, liquid chromatography (LC) [20], supercritical fluid chromatography, spectrophotometry [21], NMR spectrometry and IR spectrometry GC–MS are available [22]. Diverse treatments for eliminating IBU have been proposed, for instance, adsorption on activated carbon, microbial biofilm, biological and physical membrane processes, as well as advanced oxidation processes (AOPs) [23,24]. Among these treatments, AOPs have been widely published in articles devoted to degradation and removal of pharmaceuticals from aqueous environment [25]. In these methods, rapidly reacting, sensitive and non-selective oxidizing species such as hydroxyl radicals are formed, which may oxidize most of the organic matter in water. They are most assuring methods for the removal of pharmaceutical waste products found in water [4]. Furthermore, elimination processes of IBU by AOPs heave been published, for instance by utilizing photo-Fenton, photocatalytic, ultrasound and Fe-based catalysts [26–28]. Ozonation is a widely employed technology for drinking water treatment. These methods are very attractive and, in the vast majority of cases, they transform pollutants into harmless products, including strong oxidizing properties, disinfection potential, and very low selectivity, hence allowing the treatment of a wide range of contaminants. Ozonation has other benefits such as the ability to eliminate a pungent smell. Under the conditions of water treatment, ozone produces hydroxyl radicals. Ozone is an electrophilic molecule and it especially reacts with high electronic density sites of molecules such as organic compounds having carbon–carbon double or triple bonds and aromatics [1,29].

The ozonation process has some confines such as difficulty in eliminating by-products, the low ozone solubility and the stability in water, as well as the selective reactions between ozone and pollutants. Some oxidation processes are slow, while some are incomplete. For this reason, to develop the ozonation process further, it is applied in combination with heterogeneous catalysts to improve the decomposition of ozone and production of hydroxyl radicals [30]. For the removal of organic compounds, such as pharmaceuticals, heterogeneously catalyzed ozonation has been applied [31]. Among heterogeneous catalysts, zeolites have excellent thermal and chemical stabilities in the presence of ozone and therefore they are the more assuring catalysts for long-term ozonation processes [32]. The degradation of IBU by catalysts has been reported in papers such as Fe-based catalytic ozonation with ultrasound and combination of photocatalysis and sonolysis [27,33].

In the present work, non-catalytic and heterogeneously catalyzed ozonation processes have been applied on the degradation of IBU from aqueous solutions. H- and Fe-modified Beta zeolite catalysts were used in a tailored semibatch reactor. In order to optimize the degradation process, five experimental parameters were investigated: temperature, type and position of stirrer, initial concentration of IBU, pH and gas flow rate. The influence of the catalyst amount and the Fe loading on the catalyst were studied.

2. Experimental section

2.1. Chemicals

IBU ($C_{13}H_{18}O_2$, MW:206.28 g/mol, CAS number:15687-27-1, > 98% purity) was provided in solid state by Sigma Life Science (China). Ethanol (C_2H_6O, MW: 46.06 g/mol, CAS number: 64-17-5, > 96% purity) was provided by Altia (Finland). HPLC grade methanol (H_3COH, MW:32.04 g/mol, CAS number:67-56-1) provided Vwr Prolabo Chemicals (France) and orto-phosphoric acid 85% (H_3PO_4, MW:98 g/mol, CAS:7664-38-2) were used. For the analysis of the concentration of ozone in the aqueous samples, potassium indigo tri-sulfonate ($C_{16}H_7K_3N_2O_{11}S_3$, MW:616.72 g/mol, CAS number:67627-18-3) obtained from Sigma-Aldrich (USA), sodium phosphate monobasic (H_2 NaO4P, MW: 119.98 g/mol, CAS number:7558-80-7) provided from Sigma life science (Germany) and orto-phosphoric acid were used and dipropyl-*p*-phenylenediamine (DPD) provided from Merck KGaA (Germany). For the determination of ozone in gas phase, potassium iodide (KI, MW:166 g/mol, CAS number:7681-11-0) was provided from Merck KGaA(Germany), disodium hydrogen phosphate (Na_2HPO_4*$2H_2O$, MW:177.99 g/mol, CAS number:10028-24-7) obtained from Sigma-Aldrich (Germany), potassium dihydrogen phosphate (H_2KO_4P, MW:136.09 g mol^{-1}, CAS number:7778-77-0) was provided from Fluka (Switzerland).

2.2. Catalyst preparation

Three different heterogeneous catalysts, H-Beta-25, Fe-H-Beta-EIM-25 and Fe-H-Beta-SSIE-150 were synthesized. The originate zeolites were provided by Zeolyst International. The H-Beta-25 synthesis was done by ion exchange to the form of NH4-Beta-25 by mixing Na-Beta-25 and NH_4Cl at the equimolar ratio in distilled water for 24 h [34]. The H-Beta-25 synthesis was done by the evaporation-impregnation (EIM) method, by stirring the mixture of a ferric nitrate solution and the support for 24 h at 60 °C [35]. The Fe-H-Beta-SSIE-150 was prepared by the solid-state ion exchange method (SSIE) by ball-milling the mixture of the support and iron for 8 h [36]. Later on, these catalysts were dried at 100 °C overnight and calcined at 450 °C for 4 h.

2.3. Catalyst characterization

X-ray powder diffraction (XRD) patterns were recorded with Philips X'Pert Pro MPD using monochromatic CuKα radiation at a voltage of 40 kV and a current of 50 mA. The divergence slit was 0.25° with a fixed 20 mm mask, and the diffractograms were explained with Philips X'Pert highScore MAUD programs. The morphological features of H- and Fe modified zeolite was studied via scanning electron microscopy (SEM) on a Zeiss Leo Gemini 1530 microscope. The specific surface area and pore volume of zeolites were determined by nitrogen adsorption using Carlo Erba Sorptomatic 1900 instrument and calculated by Dubinin method. The catalysts were outgassed at 150 °C for 3 h.

The Fe particle size and structural properties of Fe-H-Beta-25-EIM-Fresh, Fe-H-Beta-25-Regenerated, Fe-H-Beta-150-SSIE-Fresh and Fe-H-

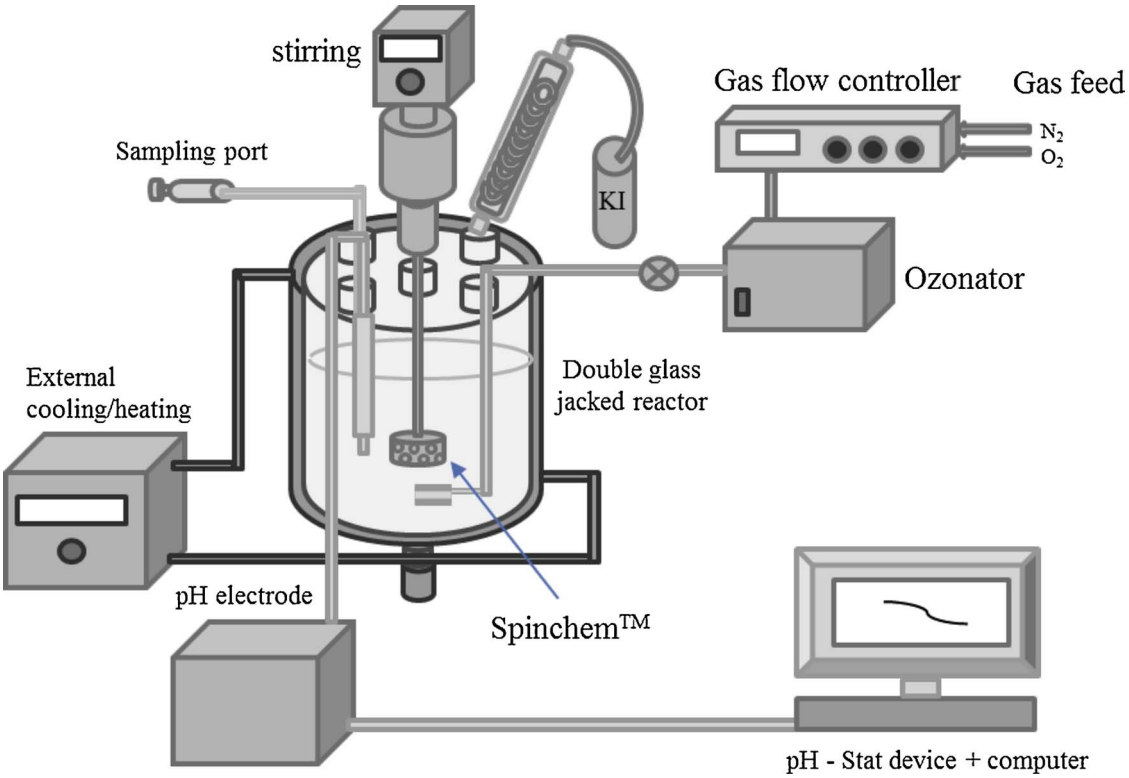

Fig. 2. Schematic presentation of the semi-batch reactor for the IBU degradation.

Beta-150-SSIE-Regenerated catalysts were measured using Transmission Electron Microscopy (TEM). The equipment used for the analyses of the Fe particles was JEM 1400 Plus with 120 kV accelerating voltage and a resolution of 0.38 nm equipped with OSIS Quemesa 11 Mpix digital camera. The average Fe particle size and distributions were calculated by counting several particles from the transmission electron micrographs.

2.4. Kinetic experiments in semi-batch reactor

To investigate the degradation of IBU, semi-batch experiments were conducted in a gas-liquid reactor system, which consisted of a double jacket glass reactor with a capacity of 1100 ml and connected to an ozone generator. Fig. 2 illustrates the reactor setup. The aqueous phase containing IBU was in batch mode, while a gas mixture containing ozone was continuously bubbled through the aqueous phase through a 7 µm disperser at the bottom of the reactor. The gas and liquid phases were exposed to vigorous stirring. Typical operating conditions were: concentration of IBU: 10–100 mg/L, gas flow: 250–1100 ml/min, the mixing rate: 250–1070 rpm, reactor temperature: 5–30 °C and the reaction time 4 h. The solutions of IBU were prepared by a stock solution of IBU in ethanol (50 mg/ml) from which 10 ml was dissolved in 1000 ml deionized water, this was done due to the low solubility of ibuprofen in water. The ozone generator (Absolute Ozone, Nano model, Canada) produced approximately a 60 mg/L concentration of ozone in the gas when an oxygen gas flow rate of 0.450 L/min combined with a 0.05 L/min nitrogen gas was used. The use of a small amounts of nitrogen (0.5–10%) in the feed is reported to be necessary by the ozonator manufacturer to maintain the maximum efficiency. As nitrogen is present, it is important to have a super dry feed gas (dew point −60 °C) to prevent the formation of nitric acid, which can damage the ozonator.

The pH was measured by a pH-stat device (Metrohm Tiamo), and in some experiments (when needed), it controlled the pH by addition of 1M sodium hydroxide. The required amount (0.25–1.0 g) of catalysts was immobilized inside the Spinchem stirrer. The catalysts size were higher than 150 µm and remain nicely inside Spinchem. For the measurement of the ibuprofen concentration, pH, and dissolved ozone, samples were withdrawn before, during and in the end of the ozonation experiment.

2.5. Chemical analysis

The concentration of IBU in the samples was analyzed by an HPLC (Agilent Technologies 1100 series) equipped with a UV–vis photo diode array detector set at 214 nm, and a quaternary pump. The column used was Ultra Techsphere ODS-5u-(C18), 250 mm × 4.6 mm. The mobile phase consisted of a 70:30 mixture of methanol and 0.5% phosphoric acid (pH:1.8), flowing at 1 mL/min, sample injection volume and retention time were 20 µL and 10 min, respectively.

The concentration of dissolved ozone was determined with the indigo method. In this process, the ozone concentration in the aqueous phase can be measured by a spectrophotometer (UV–vis) at 600 nm (pH < 4). In this method, indigo trisulfate, including alone one C=C double bond reacts with the dissolved ozone in a stoichiometric and rapid process. The transformation of the absorbance vs. ozone is $-2.0 \pm 0.1 \times 10^4$ 1/M 1/cm and it is characteristic for the concentration of dissolved ozone in the range of 0.005–30 mg/L. The accuracy of the analysis is 2% or 3 µg/L for low concentrations, if a spectrophotometer is employed. Furthermore, visual methods can be used to measure 0.01 mg/L ozone [27,37]. For comparative reasons, the ozone concentration in water was measured with the dipropyl-*p*-phenylenediamine (DPD) photometric method by using a reagent test kit to compare with the indigo method. In this method, ozone reacts with potassium iodide to produce iodine that reacts rapidly with DPD to produce a pink mixture; the intensity of the pink color is proportional to ozone concentration. The intensity was measured at 515 nm with a colorimeter or a spectrophotometer. This measurement has been used for any oxidants present in water, and the method is reported in mg/L of residual ozone concentration [38,39].

The ozone concentration in the gas phase was measured by a

iodometric method [40,41]. A buffered potassium iodide solution (200 ml) was prepared from solid potassium iodide, disodium hydrogen phosphate, monopotassium dihydrogen phosphate, following ozone bubbling for a certain time, i.e. gas was dispersed through a porous sinter at the bottom of a cylindrical (20 cm high) container of the buffered KI solution. Thereafter, it was acidified and titrated with standard sodium thiosulfate. The same gas flow conditions were used as in the kinetic degradation experiments.

3. Results and discussion

3.1. Catalyst structure and surface properties

3.1.1. X-ray powder diffraction (XRD)

XRD was used to determine the phase purity and structure of the H-Beta-25, Fe-H-Beta-25-EIM and Fe-H-Beta-150-SSIE zeolite catalysts. The X-ray powder diffraction diagrams of the Fe-H-Beta-25-EIM, Fe-H-Beta-25-SSIE zeolite catalysts exhibited typical patterns to that of pure H-Beta zeolite, indicating that the modification of Beta zeolite with Fe by using the evaporation impregnation and solid state ion-exchange methods in the catalyst preparation did not influence structure. The X-ray powder diffraction patterns of Fe-H-Beta-25-EIM and Fe-H-Beta-150-SSIE catalysts are displayed in Fig. 3.

3.1.2. Scanning electron microscopy (SEM)

SEM was used to study the morphology of the H- and Fe modified zeolite catalysts, i.e. the crystal shape, size, and crystal distribution. The smallest and largest crystallite sizes of H-Beta-25, Fe-H-Beta-EIM-25 and Fe- H-Beta-150-SSIE were (79.83, 232.8), (71.55, 468.0), (69.89, 355.4) nm, respectively. The iron concentrations of fresh (catalyst synthesized prior to use), spent (catalyst used in the reaction) and regenerated (after calcination of spent catalyst for 2 h at 400 °C) Fe-H-Beta-EIM-25 and Fe- H-Beta-150-SSIE was (6.05%, 4.84%, 3.11%), (2.99%, 2.5%, 1.94%), respectively. Uniform and regular spherical particles of diverse sizes are visible in the SEM micrographs. The SEM of Fe-H-Beta-EIM-25 fresh, spent and regenerated samples are presented in Fig. 4. The SEM images of spent and regenerated zeolites confirm that they did not undergo any morphological changes during the degradation of IBU or during the regeneration of the spent catalyst.

3.1.3. Transmission electron microscopy (TEM)

The Fe particle size, distributions and structure were analyzed with TEM. The transmission electron micrographs exhibited the typical uniform porous structures of the Beta zeolite. It is significant to mention that the methods of Fe modifications such as evaporation impregnation (EIM) and solid state ion-exchange (SSIE) did not influence the basic porous structures of the Beta zeolites. The transmission electron micrographs of Fe-H-Beta-25-EIM, Fe-H-Beta-150-SSIE are shown in Fig. 5a–d, along with the Fe particle size distributions.

The Fe particle size distributions were determined for the fresh and regenerated Fe-H-Beta-25-EIM and Fe-H-Beta-150-SSIE catalysts, respectively. The Fe particle size distributions are given in the forms of histograms Fig. 6a–d. The histogram for the Fe-H-Beta-25-EIM-Fresh catalyst shows Fe particles size distributions within the range of 6–30 nm (Fig. 6a). However, the Fe-H-Beta-25-EIM-Regenerated exhibited much broader Fe particle size distributions of 6–70 nm (Fig. 6b). The explanation for the broad distributions for the Fe particles size for the regenerated catalyst can be attributed to the thermal treatment of the catalyst during the calcination procedure. The Fe-H-Beta-150-SSIE-Fresh catalyst prepared by using solid-state ion-exchange method showed Fe particle size distributions between 8–50 nm (Fig. 6c), however the Fe-H-Beta-150-SSIE-Regenerated catalyst exhibited Fe particle size distribution 8–30 nm (Fig. 6d).

3.1.4. Nitrogen physisorption

The specific surface areas of the catalysts were determined by the nitrogen adsorption- desorption. Table 1 shows the specific surface areas of the proton form zeolites and iron-modified zeolite catalysts. The proton form of the H-Beta-25 catalyst (fresh) showed a higher surface area than the Fe-H-Beta-25-EIM and Fe-H-Beta-150-SSIE zeolite catalysts. The reason for the decrease of the surface areas for the Fe modified Beta zeolite catalysts as compared to the proton form Beta zeolite could be the partial blockage of the pores with large particles of Fe°, FeO, Fe_2O_3. The highest surface area (1068 m^2/g) and pore volume (0.379 m^2/g) was measured for the pristine H-Beta-25 catalyst (Table 1).

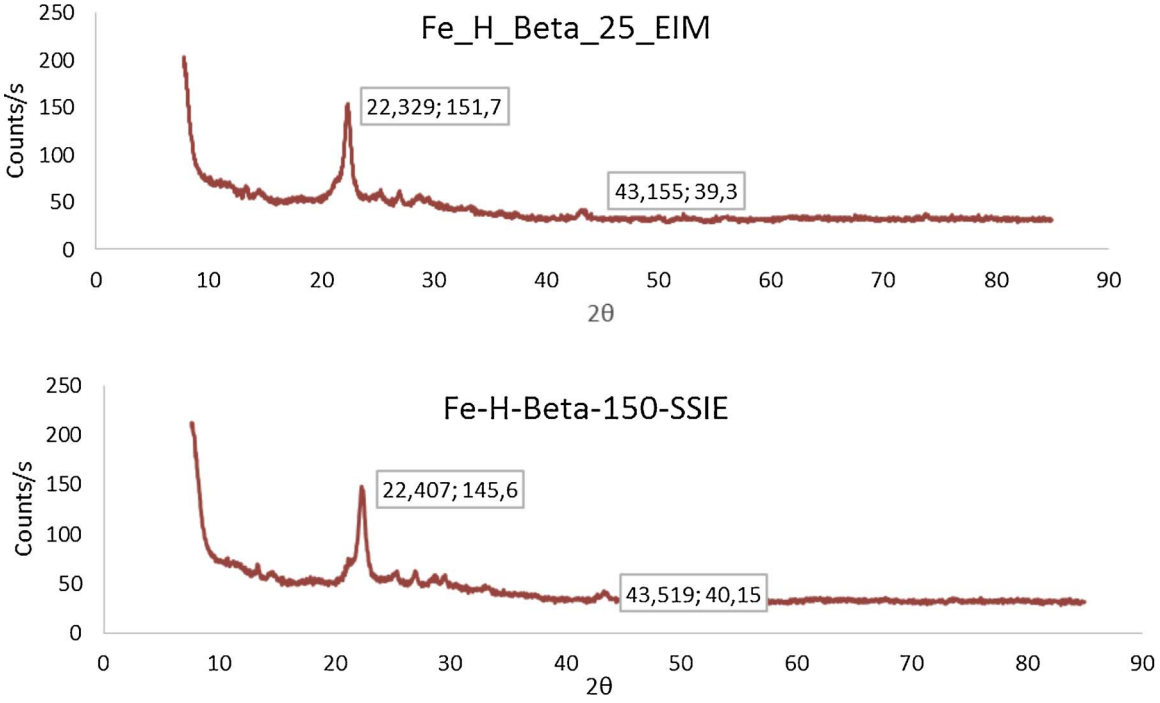

Fig. 3. X-ray powder diffraction patterns of Fe-H-Beta-EIM-25 and Fe- H-Beta-150-SSIE catalysts.

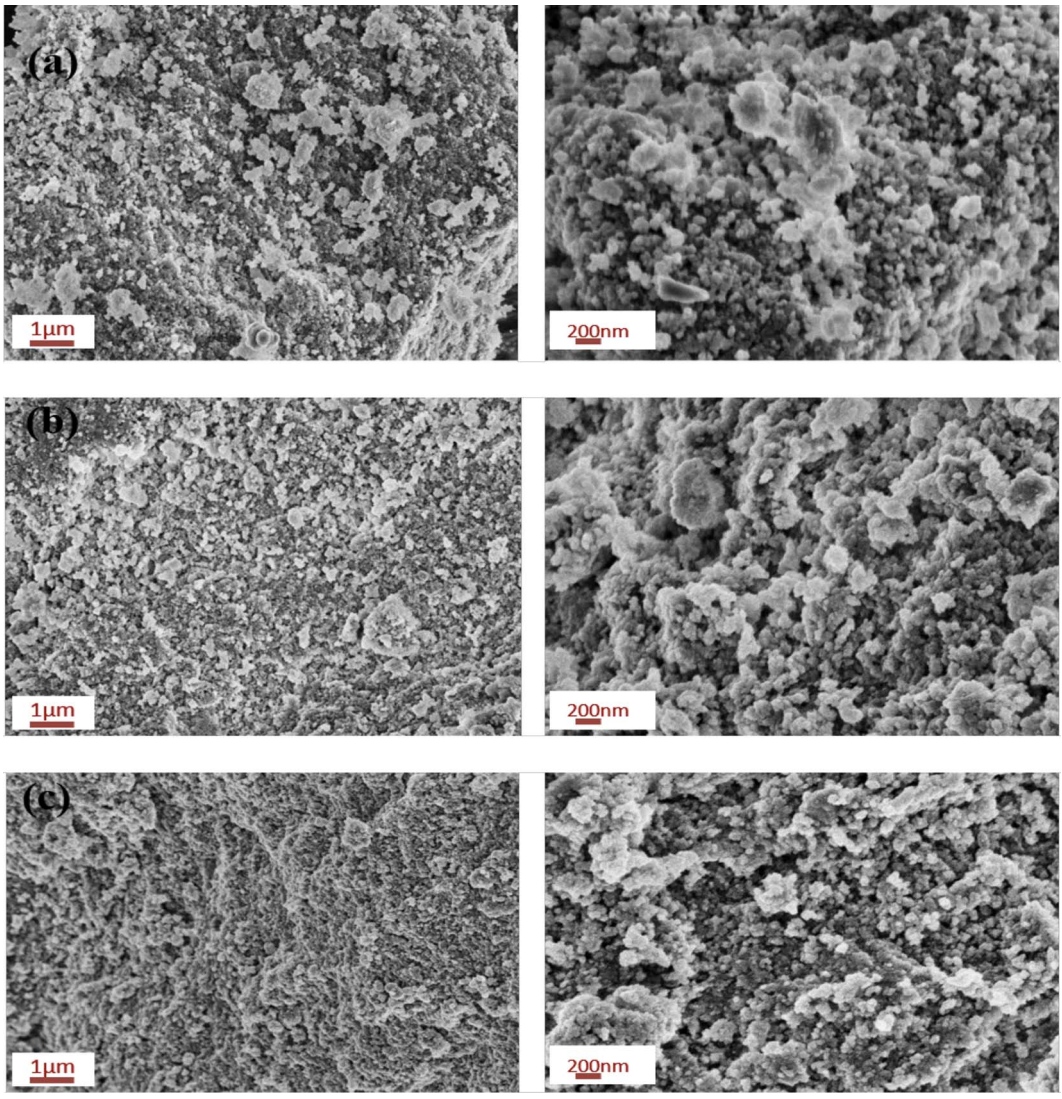

Fig. 4. Scanning electron micrographs of **a** fresh, **b** spent, **c** regenerated of Fe- H-Beta-25-EIM (left = 10000×; right = 25000×).

The H-Beta-25 (226 m^2/g), Fe-H-Beta-25-EIM (242 m^2/g) and Fe-H-Beta-150-SSIE (486 m^2/g) spent catalysts exhibited lower surface areas and pore volumes than their fresh counterparts (Table 1). The plausible explanation for the decrease of the surface area and pore volume of the spent catalysts is the coke formation in the pores of the catalysts. However, it is noteworthy to mention that in the case of all the three spent catalysts, regeneration was possible by using step calcination procedure and substantial surface area and pore volume were recovered, H-Beta-25-Regenerated (609 m^2/g), Fe-H-Beta-25-EIM-Regenerated (440 m^2/g, Fe-H-Beta-SSIE- Regenerated (537 m^2/g) (see Table 1). The best recovery was achieved with the Fe-H-Beta-SSIE-150 catalyst, whose specific surface only decreased 5% after the regeneration.

3.1.5. Pyridine adsorption-desorption with FTIR spectroscopy

The amount of Brønsted and Lewis acid sites of the proton form and Fe modified zeolites have been determined by FTIR using pyridine as the probe molecule. The activities of the catalysts used in this work are summarized in (Table 2). The Brønsted acidity increases with an increasing alumina content [42,43]. The largest amount of Brønsted acid sites was determined for the pure H-Beta-25 zeolite catalyst (Table 2). It was observed that the strong Brønsted and Lewis acid sites (450 °C) decreased substantially for the Fe-H-Beta-25-EIM and Fe-H-Beta-150-SSIE as compared to the pristine H-Beta-25 catalyst.

3.2. Primary experiments to increase the amount of dissolved ozone in the aqueous phase

The purpose of the preliminary experiments was to find the optimal conditions to achieve the maximum ozone concentration and the best ozone mass transfer into the liquid phase. Normally, the gas flow into the ozone generator was 500 ml/min (90% oxygen, 10% nitrogen). The ozone concentration in the gas flow was be calculated using the iodometric method. The ozone concentration was estimated from Eq. (1) as shown below [41],

$$\frac{Co_3}{(g/L)} = \frac{24*\text{volume of thiosulfate (L)}*\text{Normality of thiosulfate}}{\text{inlet volume of gas passed (L)}}$$

For example, for a gas flow of 500 ml/min and 1 min bubbling, the concentration of ozone in the gas feed to the reactor was calculated accordingly,

$$\frac{24*12.5\,\text{mL}*0.1}{500\text{ml}} = 0.06\left(\frac{\text{g}}{\text{L}}\right)$$

which equals 60 mg/L of ozone in the gas phase.

Concerning the concentration of ozone in the aqueous phase, the PDP method was found out to be inconsistent at different temperatures and values of pH. Therefore, the values obtained with the indigo method were preferred.

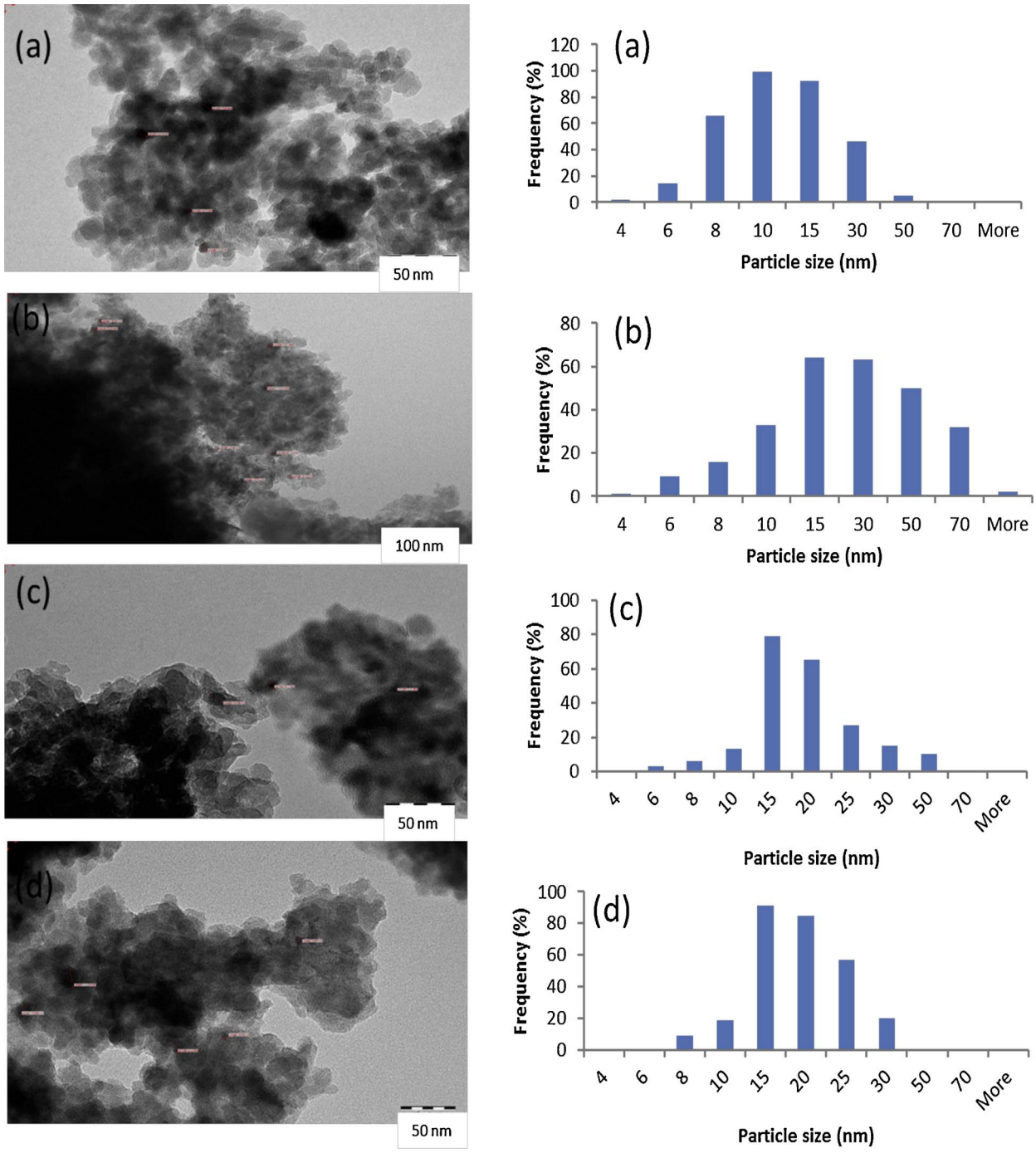

Fig. 5. HR-TEM images and Fe particle size distribution histograms of **a** fresh, **b** regenerated of Fe- H-Beta-25-EIM, **c** fresh and **d** regenerated of Fe- H-Beta-150-SSIE.

3.2.1. Influence of temperature on the concentration of dissolved ozone (indigo method)

The effect of the reaction temperature (5–30 °C) on the ozone solubility was investigated without any reactants present. Fig. 6 illustrates how gas-liquid mass transfer and the solubility of ozone was influenced the different gas flows of 500, 750, 1000 ml/min, at different temperatures using a standard four-blade stirring rod. The experiment reveals that the ozone concentration decreased at higher temperatures in all of the experiments. When decreasing the temperature to 5 °C, the highest ozone concentration was observed, which ranges from approx. 3–6 mg O_3/L at 500–1000 mL/min gas flows.

3.2.2. Influence of gas flow velocity on the concentration of dissolved ozone

Fig. 7 illustrates how the solubility of ozone changed at different temperatures (5, 10, 15 °C) and different gas flows. The results reveal that the ozone concentration is increased linearly in higher gas flow rates in all the experiments. In this work, in terms to approach economical feasibility, the gas flows were fixed to 500 ml/min in the subsequent experiments. The ozone concentration did not increase noticeable with long period ozonation (more than 1 h) at same condition.

Similar results have been obtained by J. Leusink [44], who reported that a lower temperature and higher ozone concentration in the inlet gas leads to a higher dissolved ozone concentration.

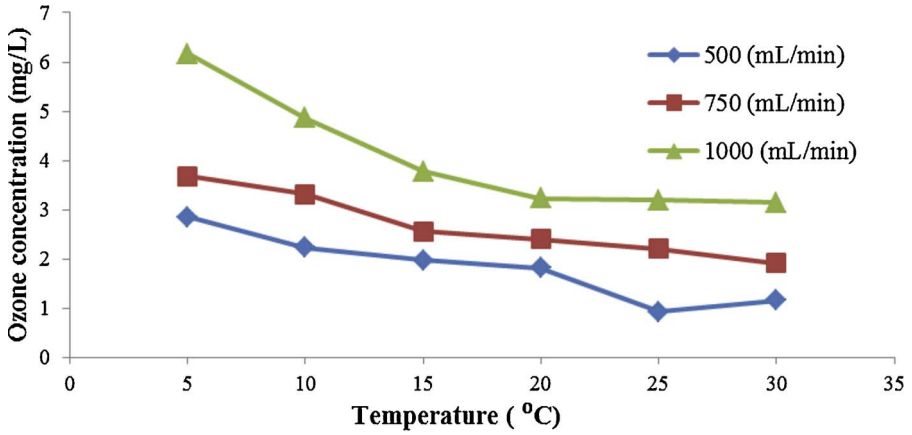

Fig. 6. Effect of temperature on the ozone concentration in the aqueous phase. Stirring speed = 1070 rpm, volume = 1100 ml, ozonation period = 60 min.

Table 1
Specific surface areas and pore volumes of proton and Fe modified Beta zeolites.

Catalyst	Specific surface area (m^2/g)			Pore specific volume (cm^3/g)		
	fresh	spent	regenerated & recovery	fresh	spent	regenerated
H-Beta-25	1068	226	609/−43%	0.379	0.0802	0.2161
Fe-H-Beta-EIM-25	953	242	440/−54%	0.222	0.0858	0.156
Fe-H-Beta-SSIE-150	567	486	537/− 5%	0.216	0.1727	0.1908

Table 2
Brønsted and Lewis acidities of proton and Fe modified Beta zeolites reported in literature [31,32].

Catalysts	Brønsted acidity (μmol/g)	Lewis acidity (μmol/g)				
	250 °C	350 °C	450 °C	250 °C	350 °C	450 °C
H-Beta-25	219	187	125	82	43	25
Fe-Beta-EIM-25	216	168	17	95	36	5
Fe-Beta-SSIE-150	193	137	45	119	41	4

3.2.3. Influence of the stirrer on the concentration of dissolved ozone

The effect of different stirrer types on the dissolved ozone concentration was investigated. A normal four-blade stirrer and Spinchem™ rotating bed stirrer were used in these experiments. The comparison in Fig. 8 illustrates that the ozone concentration was significantly higher (40%) with the Spinchem stirrer, i.e. 4.15 mg/L at maximum 1070 rpm vs 2.95 mg/L. Therefore, the Spinchem stirrer was used in subsequent experiments. These experiments also confirmed that the stirring speed did not influence significantly the ozone concentration within the range of 450–1070 rpm. It is evident as also reported by Jenkins [45] that the stirring speed has a minor effect on the ozone decomposition in the reactor. The experiments demonstrated that only a small increase in the dissolved ozone concentration was achieved within the. normal stirring speed range of 400–900 rpm.

3.3. Non-catalytic degradation of ibuprofen

3.3.1. Influence of different gas flow rates on the oxidation of ibuprofen

The degradation of ibuprofen at several inlet gas flow rates was investigated. The results are depicted in Fig. 9. The decomposition rate of IBU increases with higher inlet gas flow rates until 500 ml/min. However, there is hardly any difference between 500 ml/min and 1000 ml/min. Probably 500 ml/min gas flow rate seems to be enough for IBU degradation. Therefore, higher flow rates were not used in the later experiments, in order to save in the gas consumption in the laboratory experiments.

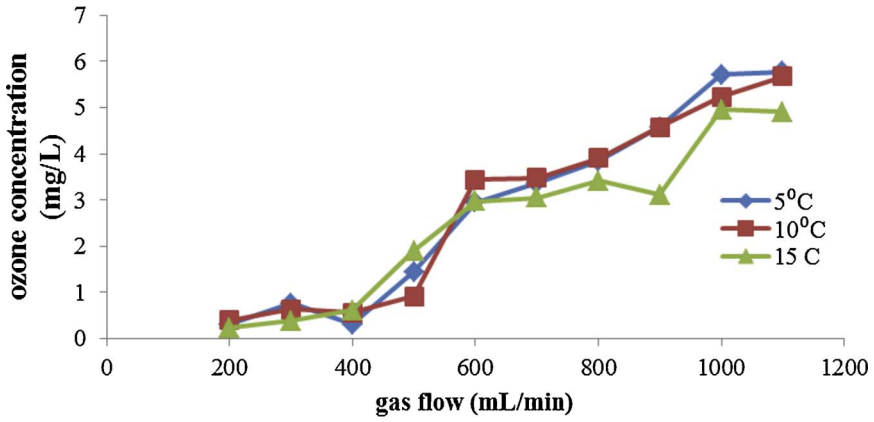

Fig. 7. Effect of the gas flow rate on the ozone concentration in the aqueous phase. Stirring speed = 1070 rpm, volume = 1100 ml, ozonation period = 135 min.

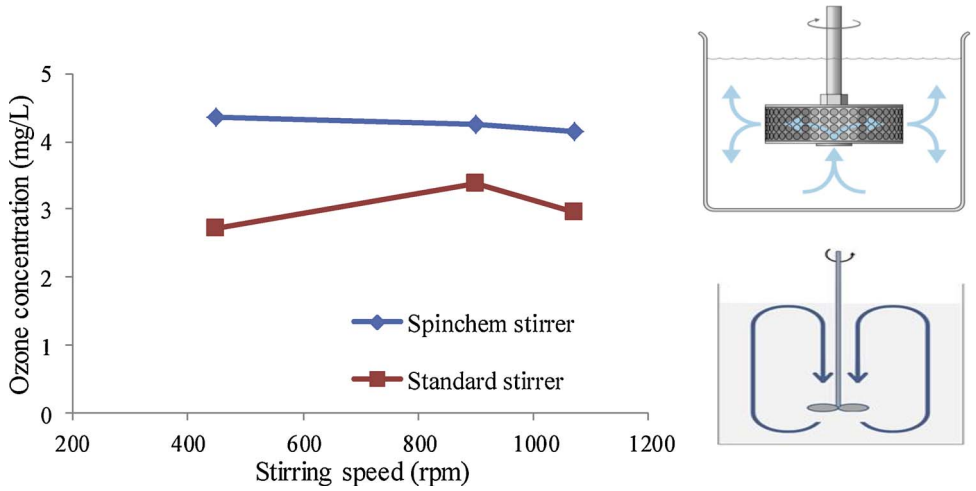

Fig. 8. Effect of stirring type and stirring speed on the ozone concentration in the aqueous phase. T = 5 °C, volume = 1100ml, gas flow = 500 ml/min, ozonation period = 60 min, stirring speeds 450, 900 and 1070 rpm.

3.3.2. Influence of scavengers on the samples

The residual ozone in the samples withdrawn from primary experiments was quenched by helium or ultrasound. Samples analyzed immediately with the HPLC were compared with samples treated with ultrasound or helium. There was not any visual difference between with or without helium and ultrasound treatment of the samples. Consequently, in further experiments no scavenging method was employed.

3.3.3. Influence of different temperatures during the oxidation of ibuprofen

The non-catalytic degradation of ibuprofen at several temperatures is illustrated in Fig. 10 The decomposition rate of IBU was most prominent during the first two hours, after which there is only a minor difference in the experiments conducted at different temperatures. IBU was not degraded quantitatively in the experiments, which indicates that the reaction order is 1 or higher with respect to IBU (Fig. 11).

3.3.4. Influence of the position of the stirrer

In this series of experiments, the Spinchem™ stirrer was placed at different vertical levels of the reactor and the IBU concentration was investigated as a function of reaction time. The results revealed that as the stirrer was placed at the lowest level of the reactor, IBU was decomposed at the highest rate. This is due to the fact that a better mass transfer was obtained when the stirrer was placed at as low level as possible, above the gas disperser due to fact that gas bubbles are forced through the Spinchem rotating bed, and further dispersed to smaller bubbles, and moreover, the residence times of the bubbles are prolonged.

3.3.5. Influence of the initial concentration of IBU

The effect of the initial IBU concentration ranging between 10–30 mg/L was investigated. These kind of experiments reveal the decomposition kinetics as illustrated in Fig. 12. Normalizing the experimental the data to dimensionless concentrations was helpful as it allows the experiments conducted with different initial concentrations of IBU to be compared in the same plot. Fig. 12b shows that the experiments with different initial concentrations of IBU overlap, which indicates first order kinetics with respect to IBU. On the other hand, the IBU concentration tends to remain on a plateau level at higher reaction times, which indicates a somewhat higher reaction order as the reaction progresses. Aziz et al. have reported similar kinetics for the degradation of IBU by direct ozonation [4].

3.3.6. The difference on the reactant (IBU) form

The degradation rates of IBU and the sodium salt of IBU were measured and compared. IBU cannot be easily dissolved in water. In this research, ethanol was used for to dissolve IBU in water, but the

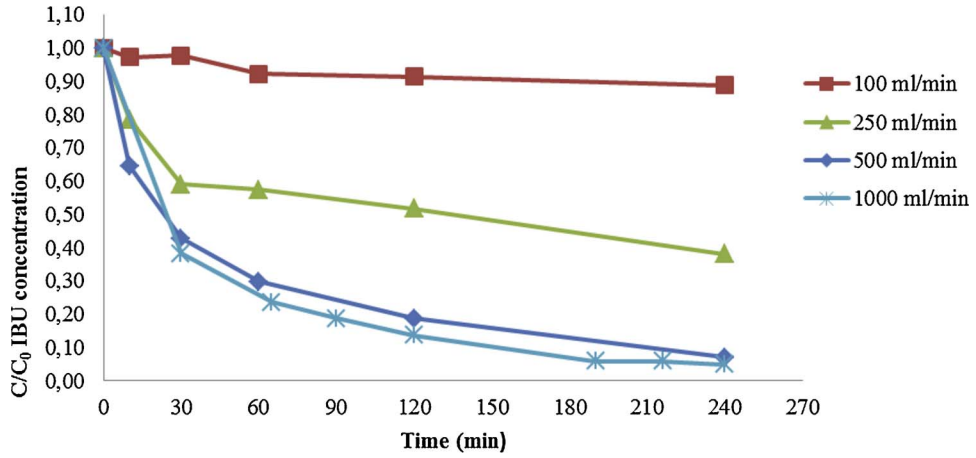

Fig. 9. The degradation of IBU by ozonation at different inlet gas flow rates. Initial concentration of IBU = 10 mg/L, T = 25 °C, stirring speed = 1070 rpm, volume = 1000 ml.

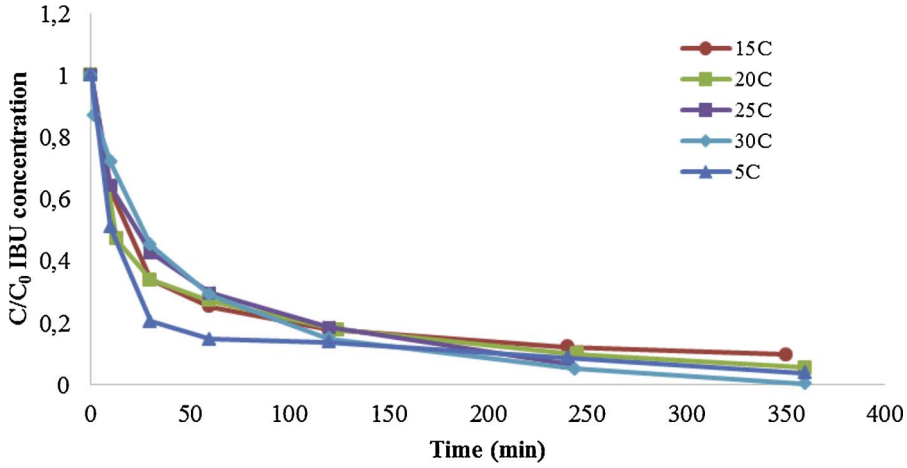

Fig. 10. The degradation of IBU by ozonation at different temperatures. Initial concentration of IBU = 10 mg/L, T = 5 °C–30 °C, stirring speed = 1070 rpm, volume = 1000 ml, gas flow = 500 ml/min.

solubility of the IBU sodium salt (IBUNa) is thousand-fold higher in water than the solubility of normal IBU, which enabled us to perform experiments with much larger initial reactant concentrations. IBUNa reacted somewhat slower than IBU as indicated by Fig. 13. Different initial concentrations of IBUNa were investigated and the results are compared in Fig. 14. The normalized plot (Fig. 14b) shos that the normalized concentration decreases more rapidly with an increasing initial concentration, which is characteristic for reaction orders exceeding 1.

3.3.7. Degradation of ibuprofen by ozonation with varying pH

The formation of various kinds of radicals is highly influenced by the pH of the aqueous solution. By a constant addition of NaOH, the pH level of the reactant solution can be maintained at a desired level. Therefore, it can be concluded that ozone and NaOH react together, probably forming radicals and other components, i.e. molecular oxygen, which is indicated by the consumption of alkaline. The effect of pH in the chain reaction of ozone in the initial step is presented and herein, hydroxide ions and ozone reaction produce a superoxide anion $O_2^{\bullet -}$ and a hydroxyl radical $HO_2^{\bullet}$.

$$O_3 + OH^- \rightarrow O_2^{\bullet -} + HO_2^{\bullet} \quad k_1 = 70\ 1/M\ 1/s$$

This means that ozone decomposes by the hydroxide ion, which acts as a catalyst towards decomposition. In the second step, ozone dissociates in the presence of $HO_2^{\bullet}$ and $O_2^{\bullet -}$. Further chain reaction produces $O_3^{\bullet -}$and $HO_3^{\bullet}$ which results the formation of $HO^{\bullet}$. These radicals could react with organic compounds and ozone itself [46]:

$$O_3 + O_2^{\bullet -} \rightarrow O_3^{\bullet} + O_2 \quad k_2 = 1.6 \times 10^9 1/M\ 1/s$$

$$HO_3^{\bullet} \leftrightarrow O_3^{\bullet -} + H^+ \quad pK_a = 6.2$$

$$HO_3^{\bullet} \rightarrow OH^{\bullet} + O_2 \quad k_3 = 1.1 \times 10^5 1/M\ 1/s$$

Without controlling the pH, the pH level of the reaction medium tends to decrease rapidly to approximately pH = 3, independent of any reactant is present or not. Fig. 15 illustrates that the decomposition rate of IBU dramatically decreases at higher pH. The reason for the decrease of pH can probably be the formation of small amounts of nitric acid in the ozonation.

The formation of nitric acid is possible if the feed gas contains nitrogen and minor amounts of moisture is present in the ozonator. Nitric acid was plausibly identified (same retention time as HNO_3) as a growing peak in the standard HPLC analysis when using 10% N_2 in the feed gas. Probably, the N_2 gas in the line contains some minor humidity, which could accumulate over a prolonged time. However, comparative experiments were carried out with either pure oxygen feed gas or including 10% nitrogen to the feed, and the results are ruled out that the small amounts of nitric acid could influence on the kinetics of the degradation of IBU. On the other hand, Quero-Pastor reported that the optimum IBU degradation rate by ozonation was obtained at an initial pH of 9 [6]. In that study, only the initial pH was applied, whereas in our study, the pH was constantly kept at the desired level, which could explain the differences in the results.

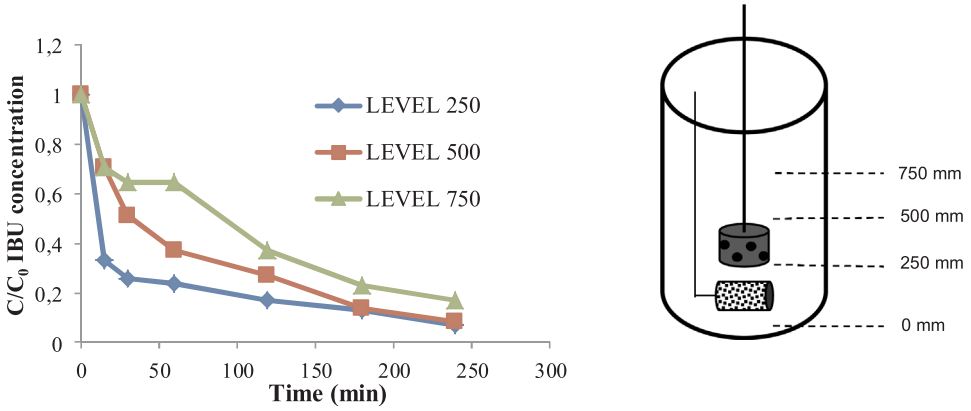

Fig. 11. The degradation of IBU at different position of stirrer by ozonation. Initial concentration of IBU = 10 mg/L, gas speed = 500 ml/min, T = 5 °C, stirring speed = 1070 rpm, volume = 1100 ml.

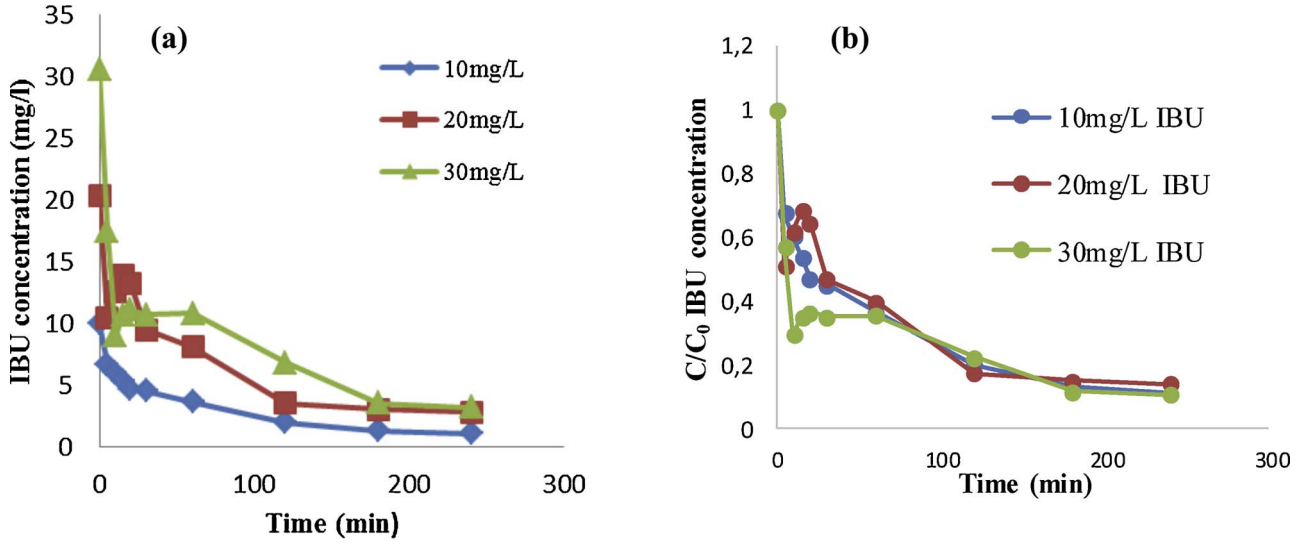

Fig. 12. a) The degradation of IBU at different initial concentration of IBU by ozonation. b) Normalized concentrations. [IBU] = 10, 20, 30 mg/L, gas flow rate = 500 ml/min, T = 5 °C, stirring speed = 1070 rpm, volume = 1100 ml.

3.4. Catalytic degradation of ibuprofen

In the following experiments, the combination of ozone with a solid catalyst was used for the degradation of IBU. The desired amount of the solid catalyst was inserted into the Spinchem™ compartment. After the experiments, the spent catalyst was carefully removed for further analysis. Otherwise, the experiments were following the same procedures as in the non-catalytic case. The main results are summarized here.

3.4.1. H-Beta-25 zeolite catalyst

Fig. 16 clearly reveals that the H-Beta-25 zeolite catalyst increases the degradation rate of IBU. It can be summarized that as compared to the non-catalytic degradation of IBU, the use of acidic H-Beta-25 zeolite catalyst increase the IBU degradation and degradation rate increases with increasing catalyst amount.

3.4.2. Fe-H-Beta-25-EIM catalyst

Fig. 17 demonstrates the enhancement of the degradation of IBU with the use of Fe-H-Beta-25-EIM catalyst. Additionally, this figure illustrates that the decomposition rate of IBU was higher when applying 0.5 g of the Fe-H-Beta-25-EIM catalyst.

3.4.3. Fe-H-Beta-150-SSIE catalyst

The Fe-H-Beta-150-SSIE catalyst exhibited a higher degradation of IBU compared to H-Beta-25 acidic and non-catalytic IBU degradation. The results reveal that the decomposition rate is higher when using the Fe-H-Beta-150-SSIE catalyst.

It is important to conclude, that with an increase of the amount of Fe modified (Fe-H-Beta-25-EIM and Fe-H-Beta-150-SSIE) zeolite catalysts, an enhancement in the degradation of IBU was obtained, which clearly indicates the positive role of Fe in the degradation of IBU. Furthermore, it can be stated that besides the amount of Fe-H-Beta-25-EIM and Fe-H-Beta-150-SSIE catalysts, the Fe particles size can have a substantial effect on the degradation of the IBU.

Catalytic ozonation of IBU by Fe-species has also been studied by Zilan et al. [47]. Their results showed that most of these catalysts have a positive effect to the degradation of IBU, besides the solid forms were efficient in increasing the mineralization rate. Additionally, Gomes et al. [43] investigated the Ag and Pt loading on TiO_2 during photocatalytic ozonation of emerging parabens contamination, and they

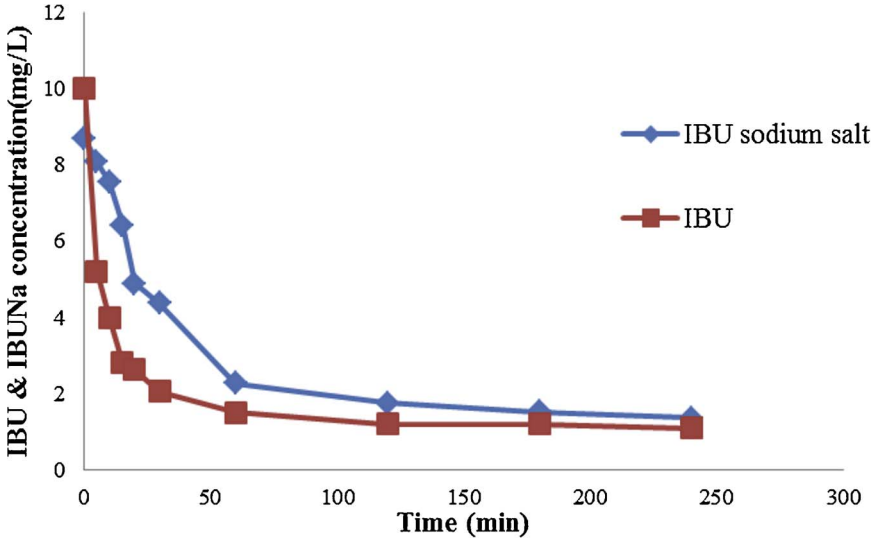

Fig. 13. The degradation of IBU and IBU sodium salt by ozonation. [IBU] = 10 mg/L, [IBUNa] = 10 mg/L, gas speed = 500 ml/min, T = 5 °C, stirring speed = 1070 rpm, volume = 1100 ml.

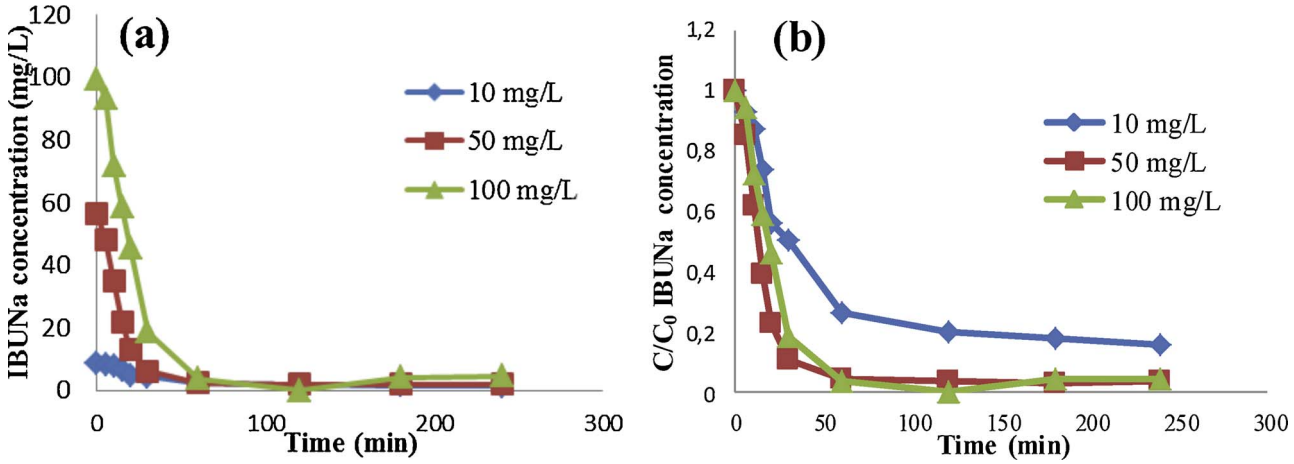

Fig. 14. (a) The degradation of IBUNa at different initial concentrations of IBUNa by ozonation. b) Normalized concentration, [IBUNa] = 10, 50, 100 mg/L, gas flow rate = 500 ml/min, T = 5 °C, stirring speed = 1070 rpm, volume = 1000 ml.

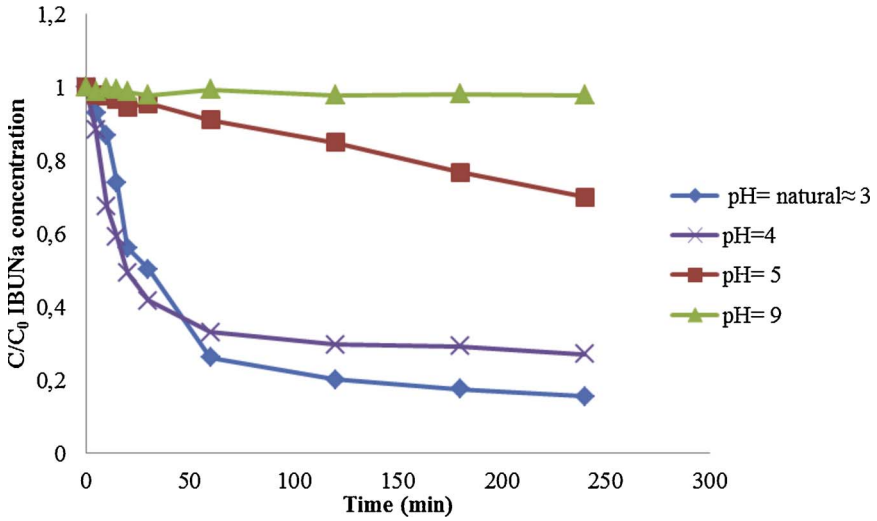

Fig. 15. The degradation of IBUNa at different pH by ozonation. [IBU Na] = 10, 20, 30 mg/L, gas flow rate = 500 ml/min, T = 5 °C, stirring speed = 1070 rpm, volume = 1000 ml.

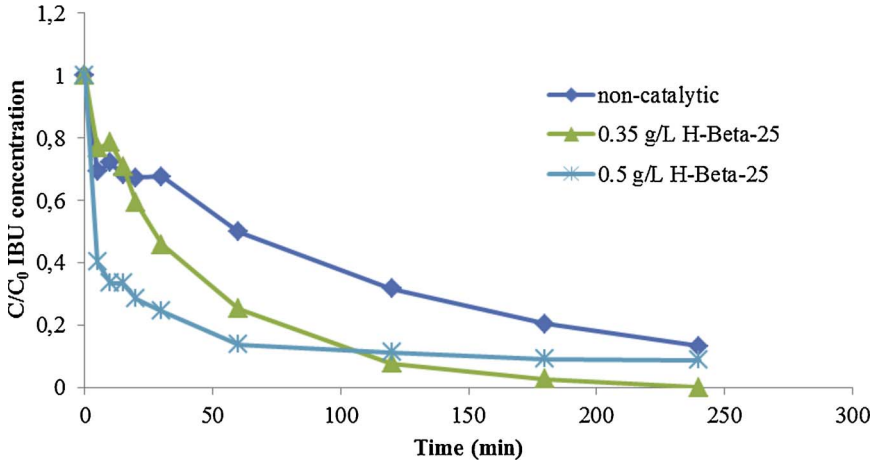

Fig. 16. The degradation of IBU by ozonation with and without H-Beta-25 zeolite catalyst. [IBU] = 10, 20, 30 mg/L, gas flow rate = 500 ml/min, T = 5 °C, stirring speed = 1070 rpm.

noticed that an increase in the metal loading doped onto TiO_2 gave increased degradation efficiency. These results are similar to our work - loading iron on zeolites results in a higher degradation rate of IBU [48]. Fig. 19 illustrates the difference of the IBU degradation by ozonation, with and without iron loaded on the zeolites.

4. Conclusions

The Fe-H-Beta-25-EIM and Fe-H-Beta-150-SSIE catalysts were synthesized by using evaporation impregnation and solid state ion-exchange methods. The X-ray powder diffraction, scanning electron microscopy and transmission electron microscopy characterization results

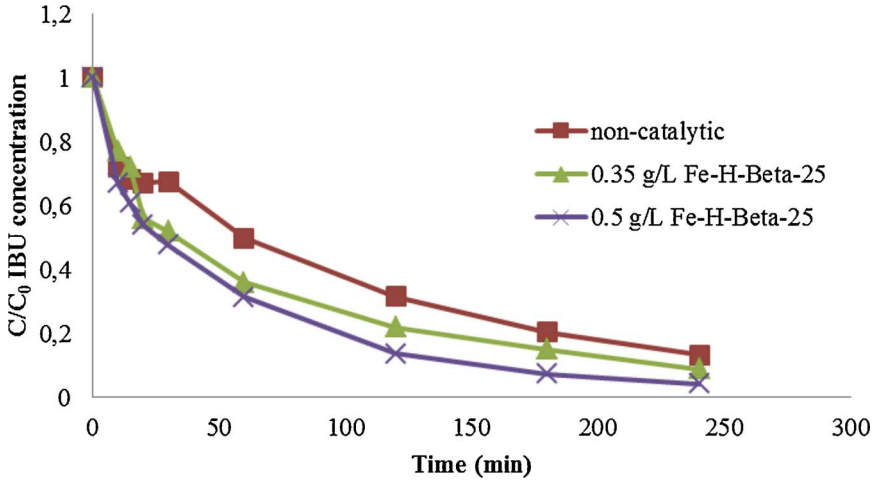

Fig. 17. The degradation of IBU by ozonation and Fe-H-Beta-EIM-25 zeolite catalyst. [IBU] = 10, 20, 30 mg/L, gas flow rate = 500 ml/min, T = 5 °C, stirring speed = 1070 rpm.

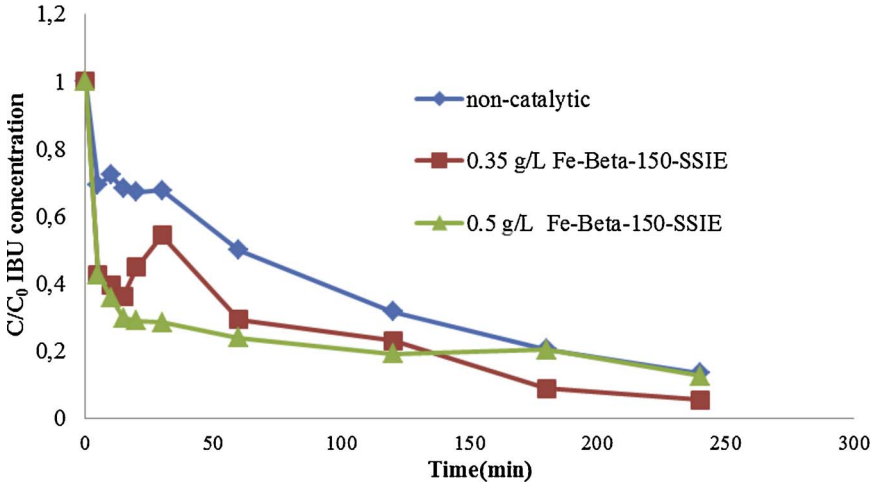

Fig. 18. The degradation of IBU by ozonation with and without Fe-H-Beta-150-SSIE zeolite catalyst. [IBU] = 10, 20, 30 mg/L, gas flow rate = 500 ml/min, T = 5 °C, stirring speed = 1070 rpm.

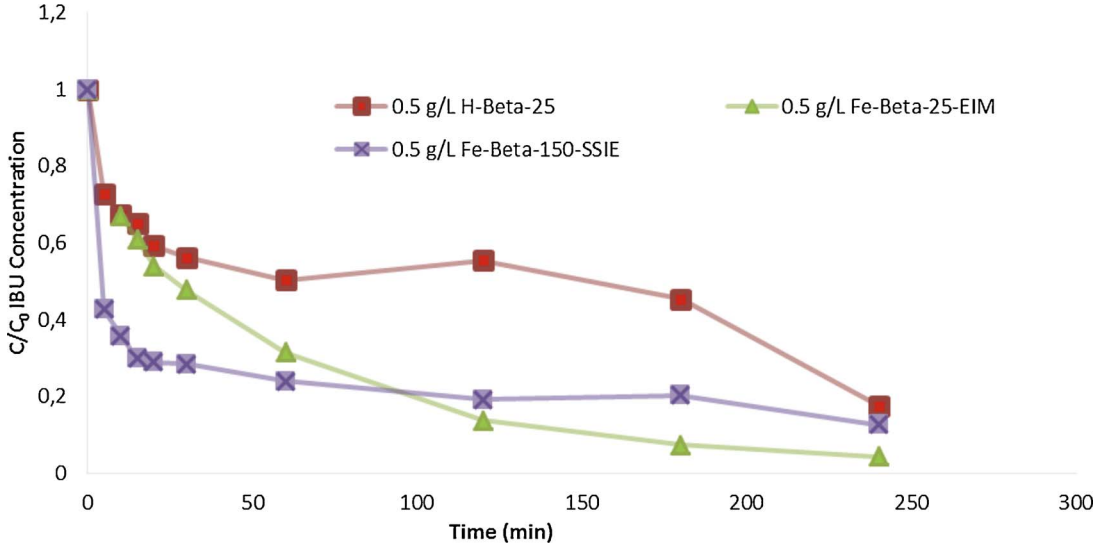

Fig. 19. The degradation of IBU by ozonation and, with and without iron loaded on zeolite. [IBU] = 10, 20, 30 mg/L, gas flow rate = 500 ml/min, T = 5 °C, stirring speed = 1070 rpm.

of these catalysts exhibited the structural integrity of Beta zeolite after Fe modifications.

Following the optimization of the experimental parameters (pH, temperature, gas flow, stirrer type and stirrer position), it was concluded that the ozone concentration is highest in water at the lower temperature (5 °C) and highest gas flow rate and using Spinchem stirrer. When Spinchem was placed at lower levels of the reactor the decomposition rate of ibuprofen was increased. The presence of zeolite catalysts improved the IBU decomposition rate significantly in the aqueous environment (Fig. 16–18).

The amount of Brønsted and Lewis acid sites in the H-Beta-25 zeolite influenced the degradation of IBU. The Fe-H-Beta-25-EIM with larger amounts of Brønsted and Lewis acid sites exhibited a higher degradation of IBU than Fe-H-Beta-150-SSIE with a smaller amount of Brønsted and Lewis acid sites. It was possible to regenerate the spent H-Beta-25, Fe-H-Beta-25-EIM and Fe-H-Beta-150-SSIE catalysts after the IBU degradation by calcination.

Acknowledgments

The work is a part of the activities of Johan Gadolin Prosess Chemistry Centre, a centre of excellence financed by Åbo Akademi. Financial support from Svenska Litteratursällskapet (SLS), Centre for International Mobility (CIMO) and Tekniikan Edistämissäätiö (TES) is gratefully acknowledged. SpinChem™ AB is gratefully acknowledged for providing the RBR equipment. In Sweden, also the Bio4Energy programme is acknowledged. Walter och Lisi Wahls Stiftelse för naturvetenskaplig forskning is acknowledged for funding the purchase of the ozonator device.

References

[1] J. Gomes, R. Costa, R.M. Quinta-Ferreira, R.C. Martins, Science of the total environment application of ozonation for pharmaceuticals and personal care products removal from water, Sci. Total Environ. (2017).
[2] U. von Gunten, Ozonation of drinking water: part II. Disinfection and by-product formation in presence of bromide, iodide or chlorine, Water Res. 37 (2003) 1469–1487.
[3] S. Saeid, M.A. Behnajady, Photooxidative removal of phenazopyridine by UV/H_2O_2 process in a batch re-circulated annular photoreactor: influence of operational parameters, Orient. J. Chem. (2015) 1211–1214.
[4] K. Hikmat Hama Aziz, H. Miessner, S. Mueller, D. Kalass, D. Moeller, I. Khorshid, M. Amin, M. Rashid, Degradation of pharmaceutical diclofenac and ibuprofen in aqueous solution, a direct comparison of ozonation, photocatalysis, and non-thermal plasma, Chem. Eng. J. 313 (2017) 1033–1041.
[5] B.A. Wols, C.H. Hofman-Caris, D.J. Harmsen, E.F. Beerendonk, Degradation of 40 selected pharmaceuticals by UV/H_2O_2, Water Res. 47 (2013) 5876–5888.
[6] M.J. Quero-Pastor, M.C. Garrido-Perez, A. Acevedo, J.M. Quiroga, Ozonation of ibuprofen: a degradation and toxicity study, Sci. Total Environ. 466–467 (2014) 957–964.
[7] H. Eskandarloo, A. Badiei, M.A. Behnajady, TiO_2/CeO_2 hybrid photocatalyst with enhanced photocatalytic activity: optimization of synthesis variables, Ind. Eng. Chem. Res. 53 (2014) 7847–7855.
[8] S. Heydari, R. Mohammadzade Kakhki, Thermodynamic study of complex formation of b-cyclodextrin with ibuprofen by conductometric method and determination of ibuprofen in pharmaceutical drugs, Arab. J. Chem. 10 (2017) S1223–S1226.
[9] K. Kang, M. Jang, M. Cui, P. Qiu, B. Park, S.A. Snyder, J. Khim, Chemical preparation and characterization of magnetic-core titanium dioxide: implications for photocatalytic removal of ibuprofen, J. Mol. Catal. A Chem. 390 (2014) 178–186.
[10] S. Mondal, K. Bobde, K. Aikat, G. Halder, Biosorptive uptake of ibuprofen by steam activated biochar derived from mung bean husk: equilibrium, kinetics, thermodynamics, modeling and eco-toxicological studies, J. Environ. Manage. 182 (2016) 581–594.
[11] A. Kruglova, P. Ahlgren, N. Korhonen, P. Rantanen, A. Mikola, R. Vahala, Biodegradation of ibuprofen, diclofenac and carbamazepine in nitrifying activated sludge under 12 °C temperature conditions, Sci. Total Environ. 499 (2014) 394–401.
[12] N.M. Vieno, T. Tuhkanen, L. Kronberg, Seasonal variation in the occurrence of pharmaceuticals in effluents from a sewage treatment plant and in the recipient water, Environ. Sci. Technol. 39 (2005) 8220–8226.
[13] J.P. Bound, N. Voulvoulis, Predicted and measured concentrations for selected pharmaceuticals in UK rivers: implications for risk assessment, Water Res. 40 (2006) 2885–2892.
[14] A. Meierjohann, J. Brozinski, L. Kronberg, Seasonal variation of pharmaceutical concentrations in a river/lake system in Eastern, Environ. Sci. Process. Impacts (2016).
[15] S. Han, K. Choi, J. Kim, K. Ji, S. Kim, B. Ahn, J. Yun, K. Choi, J. Seong, X. Zhang, J.P. Giesy, Endocrine disruption and consequences of chronic exposure to ibuprofen in Japanese medaka (Oryzias latipes) and freshwater cladocerans Daphnia magna and Moina macrocopa, Aquat. Toxicol. 98 (2010) 256–264.
[16] H. Gong, W. Chu, S. Hiu Lam, A. Lin Yu-chen, Ibuprofen degradation and toxicity evolution during Fe^{2+}/oxone/UV process, Chemosphere 167 (2017) 415–421.
[17] G. Lyons, Pharmacuticals in the enviroment: a growing threat to our tap water and wildlife, Chem. Trust (2014).
[18] A.B.A. Boxall, V.D.J. Keller, J.O. Straub, S.C. Monteiro, R. Fussell, R.J. Williams, Exploiting monitoring data in environmental exposure modelling and risk assessment of pharmaceuticals, Environ. Int. 73 (2014) 176–185.
[19] L. Xia, L. Zheng, J.L. Zhou, Effects of ibuprofen, diclofenac and paracetamol on hatch and motor behavior in developing zebra fi sh (Danio rerio), Chemosphere 182 (2017) 416–425.
[20] S. Magiera, Ş. Gülmez, Ultrasound-assisted emulsification microextraction combined with ultra-high performance liquid chromatography–tandem mass spectrometry for the analysis of ibuprofen and its metabolites in human urine, J. Pharm. Biomed. Anal. 92 (2014) 193–202.
[21] H.E. Zaazaa, E.S. Elzanfaly, A.T. Soudi, M.Y. Salem, Application of the ratio difference spectrophotometry to the determination of ibuprofen and famotidine in their combined dosage form; comparison with previously published spectrophotometric methods, Spectrochim. Acta Part A Mol. Biomol. Spectrosc. 143 (2015) 251–255.
[22] D. Tsikas, A. Arinc Kayacelebi, E. Hanff, A. Mitschke, B. Beckmann, H. Tillmann, F. Gutzki, M. Müller, C. Bernasconi, GC–MS and GC–MS/MS measurement of ibuprofen in 10-μL aliquots of human plasma and mice serum using [α-methylo-$^2H_3$] ibuprofen after ethyl acetate extraction and pentafluorobenzyl bromide derivatization: discovery of a collision energy-dependent H/D isotope effect and pharmacokinetic application to inhaled ibuprofen-arginine in mice, J. Chromatogr. B 1043 (2017) 158–166.
[23] K. Kang, M. Jang, M. Cui, P. Qiu, B. Park, S.A. Snyder, J. Khim, Journal of molecular catalysis A: chemical preparation and characterization of magnetic-core titanium dioxide: implications for photocatalytic removal of ibuprofen, J. Mol. Catal. A Chem. 390 (2014) 178–186.
[24] V.L. Gaikwad, M.S. Bhatia, I. Singhvi, Experimental and chemoinformatics evaluation of some physicochemical properties of excipients influencing release kinetics of the acidic drug ibuprofen, Chemosphere 138 (2015) 494–502.
[25] M. Tokumura, A. Sugawara, M. Raknuzzaman, Comprehensive study on effects of water matrices on removal of pharmaceuticals by three different kinds of advanced oxidation processes, Chemosphere 159 (2016) 317–325.
[26] F. Méndez-Arriaga, S. Esplugas, J. Giménez, Degradation of the emerging contaminant ibuprofen in water by photo-fenton, Water Res. 44 (2010) 589–595.
[27] A. Ziylan, N.H. Ince, Catalytic ozonation of ibuprofen with ultrasound and Fe-based catalysts, Catal. Today 240 (2015) 2–8.
[28] S.K. Ray, Y.K. Kshetri, D. Dhakal, C. Regmi, S.W. Lee, Chemistry photocatalytic degradation of rhodamine B and ibuprofen with upconversion luminescence in Ag-BaMoO 4: $Er^{3+}/Yb^{3+}/K^{+}$ microcrystals, J. Photochem. Photobiol. A Chem. 339 (2017) 36–48.
[29] M.E. Lovato, C.A. Martín, A.E. Cassano, A reaction–reactor model for O_3 and UVC radiation degradation of dichloroacetic acid: the kinetics of three parallel reactions, Chem. Eng. J. 171 (2011) 474–489.
[30] J. Wang, Z. Bai, Fe-based catalysts for heterogeneous catalytic ozonation of emerging contaminants in water and wastewater, Chem. Eng. J. 312 (2017) 79–98.
[31] A. Ikhlaq, D.R. Brown, B. Kasprzyk-Hordern, Environmental catalytic ozonation for the removal of organic contaminants in water on ZSM-5 zeolites, Appl. Catal. B Environ. 154–155 (2014) 110–122.
[32] J. Vittenet, J. Rodriguez, E. Petit, D. Cot, J. Mendret, A. Galarneau, S. Brosillon, Removal of 2, 4-dimethylphenol pollutant in water by ozonation catalyzed by SOD, LTA, FAU-X zeolites particles obtained by pseudomorphic transformation (binderless), Micropor. Mesopor. Mater. 189 (2014) 200–209.
[33] J. Madhavan, F. Grieser, M. Ashokkumar, Combined advanced oxidation processes for the synergistic degradation of ibuprofen in aqueous environments, J. Hazard. Mater. 178 (2010) 202–208.
[34] N. Kumar, P. Mäki-Arvela, S.F. Diáz, A. Aho, Y. Demidova, J. Linden, A. Shepidchenko, M. Tenhu, J. Salonen, P. Laukkanen, A. Lashkul, J. Dahl, I. Sinev, A. Leino, K. Kordas, T. Salmi, Isomerization of a-pinene oxide over iron-modified zeolites, Top. Catal. (2013) 696–713.
[35] M. Stekrova, N. Kumar, S.F. Díaz, P. Mäki-Arvela, D.Y. Murzin, H- and Fe-modified zeolite beta catalysts for preparation of trans -carveol from α-pinene oxide, Catal. Today. 241 (2015) 237–245.
[36] M. Stekrova, N. Kumar, A. Aho, I. Sinev, W. Grünert, J. Dahl, J. Roine, S.S. Arzumanov, P. Mäki-Arvela, D.Yu. Murzin, Applied catalysis A: general isomerization of α-pinene oxide using Fe-supported catalysts: selective synthesis of campholenic aldehyde, Appl. Catal. A, Gen. 470 (2014) 162–176.
[37] H. Bader, J. Hoignie, Determination of ozone in water by the indigo method, Water Res. 15 (1981) 449–456.
[38] K.A.H. Buchan, D.J. Martin-Robichaud, T.J. Benfey, Measurement of dissolved ozone in sea water: a comparison of methods, Aquac. Eng. 33 (2005) 225–231.
[39] O. Meunpol, K. Lopinyosiri, P. Menasveta, The effects of ozone and probiotics on the survival of black tiger shrimp (*Penaeus monodon*), Aquaculture 220 (2003) 437–448.
[40] R.T. Tjahjanto, D.G.R.S. Wardani, Ozone determination: a comparison of quantitative analysis methods, J. Pure App. Chem. Res. 1 (2012) 18–25.
[41] Internatonal Ozone Assosiation, Quality Assurance Committee, (1987) Revised Standardized Procedure 001/96..
[42] P. Mäki-Arvela, J. Zhu, N. Kumar, K. Eränen, A. Aho, J. Linden, J. Salonen, M. Peurla, A. Mazur, V. Matveev, D.Yu. Murzin, Solvent-free "green" amidation of stearic acid for synthesis of biologically active alkylamides over iron supported heterogeneous catalysts, Appl. Catal. A Gen. (2017), http://dx.doi.org/10.1016/j.apcata.2017.06.006.
[43] A. Aho, N. Kumar, T. Salmi, M. Hupa, D.Y. Murzin, Catalytic pyrolsis of biomass in a fluidized bed reactor: influence of the acidity of H-Beta zeolite, Process Saf. Environ. Prot. 85 (2007) 473–480.

[44] J. Leusink, Dissolved ozone vs temperature, Ozone J. (2011) (Accessed 12 December 2017), www.ozonesolutions.com/journal/2011/dissolved-ozone-vs-temperature.
[45] S.H. Jenkins, Water pollution research, eighth international conference on water pollution research, Proceedings of the 8th International Conference, Sydney, Australia, 1976, Pergamon Press, 2013.
[46] C. Gottschalk, A.L. Judy, A. Saupe, Ozonation of Water and Waste Water, Wiley-Blackwell, 2008.
[47] A. Ziylan, N.H. Ince, Catalytic ozonation of ibuprofen with ultrasound and Fe-based catalysts, Catal. Today 240 (2015) 2–8.
[48] J. Gomes, A. Lopes, K. Bednarczyk, M. Gmurek, M. Stelmachowski, A. Zaleska-Medynska, M.E. Quinta-Ferreira, R. Costa, R.M. Quinta-Ferreira, R.C. Martins, Environmental preservation of emerging parabens contamination: effect of Ag and Pt loading over the catalytic efficiency of TiO_2 during photocatalytic ozonation, Energy Procedia 136 (2017) 270–276.